Nanophotonic Three-Dimensional Microscope

Ranjith Rajasekharan, Timothy D. Wilkinson,* Philip J. W. Hands, and Qing Dai

Department of Engineering, Centre of Molecular Materials for Photonics and Electronics, University of Cambridge, 9 J.J. Thomson Avenue, Cambridge CB3 0FA, U.K.

Supporting Information

ABSTRACT: Three-dimensional (3D) optical microscopy based on integral imaging techniques is limited mainly by diffraction effects and the pitch of the microlens array used to sample the specimen. We integrate nanotechnology to the integral imaging technique and demonstrate a nanophotonic 3D microscope, where a nanophotonic lens array is used to finely sample the specimen. The resolution limitation due to diffraction is reduced by capturing images before the diffraction effects predominate and hence overcomes the bottleneck of achieving high resolution in an integral imaging 3D microscope.

KEYWORDS: Integral imaging, 3D microscope, nanophotonic lens array, carbon nanotube, liquid crystal, diffraction

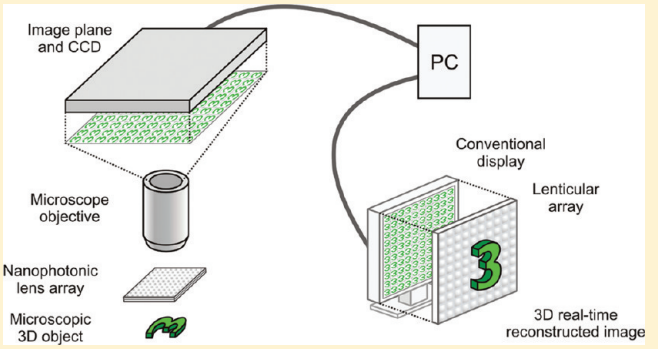

Three-dimensional (3D) microscopy can be used to reveal the shape, distribution, and connectivity of micro- and nano-sized objects.[1−8] The integral imaging technique proposed by Lippmann[9] is a 3D image display technique that produces true 3D images with full parallax and continuous viewing points. The technique also operates with regular incoherent daylight and does not need any glasses to view the 3D effect.[10−12] In the integral imaging technique, the 3D object is sampled by a lenslet array or a pinhole. Each lenslet picks up a particular perspective of the object in 2D, resulting in an array of elemental images. All the elemental images from different perspectives are recorded at a CMOS or CCD sensor. The reconstruction of the 3D image from the 2D elemental images is the reverse of the pickup process, whereby a second lens array is placed in front of a display stage or a projector.[13,14] The 3D identification of micro-objects using integral imaging techniques has attracted the attention of researchers.[15−17] The technique was first used by Jang et al.[15] and used confocal microscopy to sample the optical field at different depths. Javidi et al.[16] also used integral imaging techniques, to obtain multiviewpoint two- and three-dimensional images. An alternative technique was proposed by Lim et al.[17] In this system, displacements of the lens array provided additional sets of elemental images. This technique maintained the same field of view of the reconstructed orthographic view images, but with increased spatial density. Computational techniques can be used to further improve the resolution of final images, however, the overall resolution of the integral imaging microscope will, in all cases, be fundamentally limited by the pitch of the microlens array, diffraction, and field of view. Integral imaging cannot be applied to specimens smaller than each lenslet in the microlens array. If a lens is used to magnify such a specimen before sampling by a lens array, the 3D shape cannot be preserved because magnification will be nonuniform along the longitudinal depth direction, and thus the 3D shape cannot be preserved for a magnified image.[15] If smaller specimens are required for imaging, a possibility is to reduce the size of the lenslet. But from classical diffraction theory, as the lens size decreases, diffraction effects increase and image quality is degraded.[18] We find a solution to this problem by integrating nanotechnology to the integral imaging technique. We demonstrate a nanophotonic 3D microscope where a voltage-dependent nanophotonic lens array, based upon a nematic liquid crystal and an array of conducting multiwall carbon nanotubes, is used to sample the specimen under observation. In the nanophotonic lens array, each lenslet has a 5 μm radius which is significantly smaller than any commercially available microlens array and has 10^6 lenslets in a 10 $\times$ 10 mm area. The resolution limitation due to diffraction is reduced in the nanophotonic lens array because the short focal length (13 μm) is such that the images are captured before diffraction effects predominate. Experimental results are presented with the help of a microsized object from the standard US air force (USAF) test pattern, sampled by the nanophotonic lens array to get elemental images. Reconstructed 3D images were then made by combining all the elemental images, providing full parallax from a wide range of viewing angles.

Figure 1 shows a schematic diagram of the 3D microscope. Incoherent light from a white light source is incident upon the microsized 3D specimen object (illustrated here by the number "3"). The specimen is sampled by the nanophotonic lens array to get elemental images, followed by magnification of the elemental images using a microscope objective. The captured elemental images have different perspectives of the micro-object according

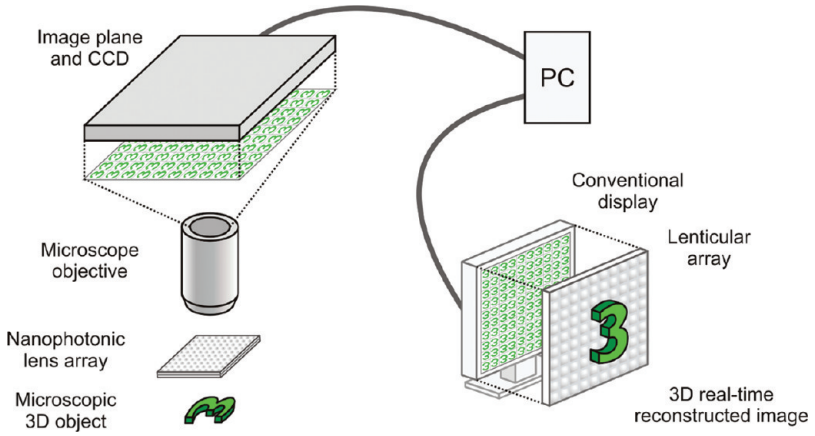

Figure 1. The schematic diagram of the nanophotonic 3D microscope. A nanophotonic lens array was used to sample the microscopic 3D object "3" to record elemental images in a CCD. The 3D image is reconstructed with full parallax using a lenticular lens array in front of an LCD where all the elemental images are displayed.

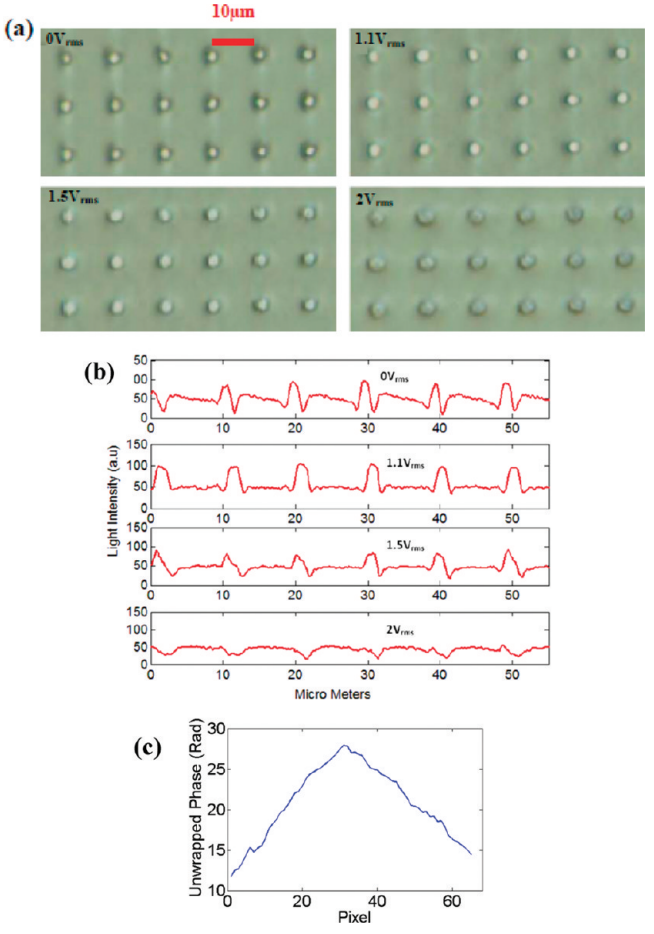

Figure 2. (a) The nanophotonic lens array focuses light at different applied voltages (a) 0 V_{rms}, (b) 1.1 V_{rms}, (c) 1.5 V_{rms}, and (d) 2 V_{rms}. (b) The one-dimensional light intensity profile across six lenslets. The focused light profile was smooth and uniform at 1.1 V_{rms}. (c) Unwrapped phase profile of a single lenslet at 1.1 V_{rms}.

to the spatial position of each lenslet. These elemental images are then recorded on a CCD. For 3D image reconstruction, the recorded elemental images are displayed by a conventional liquid crystal display (LCD). A large second lens array is then placed in front of the LCD to reconstruct the 3D image. The 3D scene with full parallax is thus reconstructed by the intersection of discrete rays coming from each elemental image.

To fabricate the nanophotonic lens array, nanotubes were grown vertically (height 3.5 μm) and periodically on quartz substrates by plasma-enhanced chemical vapor deposition, after employing e-beam lithography to a nickel catalyst layer forming an array.[19] This allowed the growth of an array of individual multiwall carbon nanotubes of around 100 nm diameter at each point in the array. The nanotubes were patterned in small groups of six with 1 μm spacing between each nanotube and 10 μm spacing between the groups. The substrate was then sputtered with a 100 nm thick layer of titanium nitride for an electrical contact across the nanotube array. The nanotube array was then assembled with a top electrode, consisting of a layer of indium tin oxide (ITO) on 0.5 mm thick borosilicate glass, to form a cell. The top electrode was also given a planar alignment for liquid crystals by spin-coating and rubbing a thin film of polyimide (AM4276, Merck). A 20 μm cell gap between substrates was set by silica spacer beads in UV-curing adhesive, and the cell was then filled with a nematic liquid crystal (BL048, Merck). Previous work has shown that when an electric field is applied between the nanotubes and the opposing ITO substrate, the spatial profile of the electric field from the nanotube is approximately Gaussian in shape.[19,20] This creates a torque in the liquid crystals about the long molecular axis, causing the molecules to align with the field (positive dielectric anisotropy). The final orientation of liquid crystal molecules within the cell is of a complex geometry due to the Gaussian field profile combined with the surface effects of the alignment layer. The result of these two effects creates a varying refractive-index profile at each nanotube site across the device, which forms a nanophotonic lens array at a particular voltage range. Panels a and b of Figure 2 show the lens array focusing light and one-dimensional light intensity profile across six lenslets at 0, 1.1, 1.5, and 2 V_{rms}. The lens array modulated light at 0 V_{rms} because the vertically grown nanotube distorts the alignment of liquid crystal molecules around the nanotube, creating a defect in the otherwise planar alignment. The refractive index profile was therefore also distorted and nonuniform across the device, giving rise to poor light focusing and imaging capability at 0 V_{rms}. At around 1.1 V_{rms}, the device acted as a lens array. At this

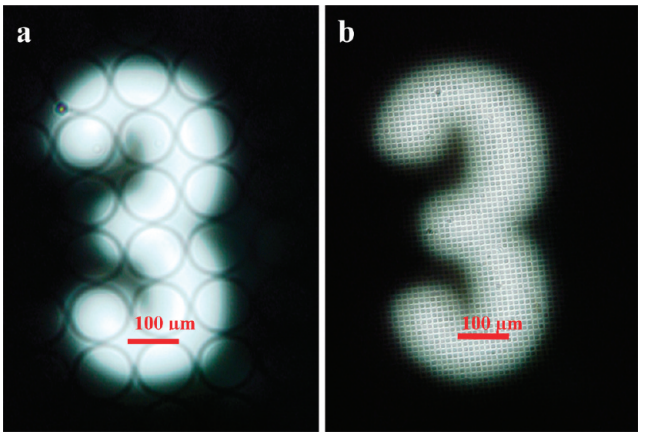

Figure 3. Microsized "3" in the US Air Force pattern sampled with (a) a standard 110 μm pitch microlens array, where the sampling was very coarse with two lenslets per object, and (b) the 10 μm pitch voltage-dependent nanophotonic lens array which gave a fine sampling with more than 20 lenslets per object.

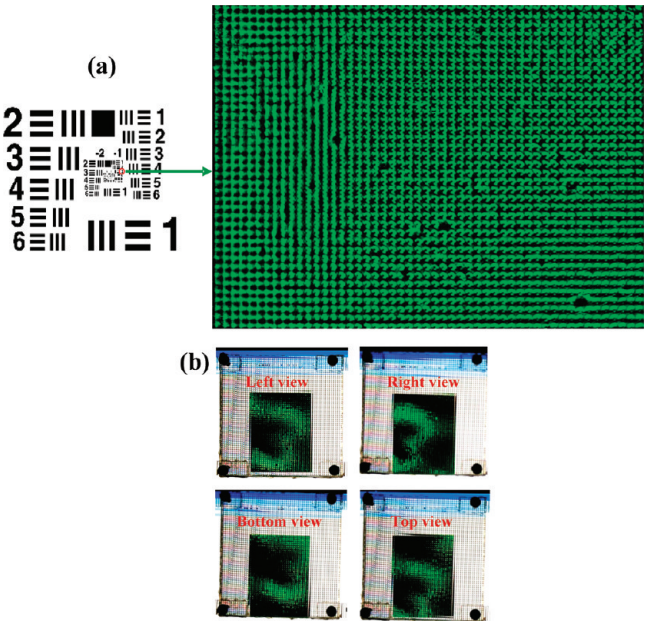

Figure 4. (a) A section of elemental images of the microsized "3" in the USAF pattern sampled by the nanophotonic lens array at 1.1 V_{rms}. (b) Reconstructed 3D images show motion parallax. The size of the 3D image is 8 cm, and the number of elemental lenses in the lens array is 60(H) × 60(V).

voltage, distortion was minimal and the light intensity was focused to a broad maximum at the nanotube positions. The light intensity was also smooth and uniform between the nanotube groups compared to other applied voltages, where the profile was noisy and less uniform. This lens-like behavior was further verified by recovering the phase profile from a single lenslet. The phase profile was quasi-parabolic as shown in Figure 2c. As the voltage increases above 1.1 V_{rms}, lens distortions begin to occur, coinciding also with increase in focal length. This is due to the effects of overlapping fringing fields, producing deviation from the ideal parabolic index profile. Above 2 V_{rms}, the liquid crystal distortion became too great for lensing to be observed.

In the nanophotonic 3D microscope, a convex lens was used to collimate the incoherent light from a white light source. The light was incident upon a specimen mounted on a sample holder. The imaging characteristics of the 3D microscope were studied using standard USAF test pattern as specimen. The specimen was kept 1 mm away from the nanophotonic lens array. The number "3" in the test pattern used for imaging had feature sizes of width 130 μm and height 550 μm. The micro-object specimen was sampled by the nanophotonic lens array, followed by magnification of the elemental images using a microscopic objective (×20 magnification). For comparison purposes, the micro-object was also sampled by a commercially available 110 μm pitch standard microlens array (Suss Micro-Optics, circular lenses, quadratic grid: lens pitch 110 μm, ROC 0.817 mm, numerical aperture 0.03, size 15 mm × 15 mm × 0.9 mm) and compared to the nanophotonic lens array in the 3D microscope. Figure 3a shows the micro-object sampled by the standard lens array where the sampling rate was very coarse and it was not possible to reconstruct a 3D image of any discernible quality. Figure 3b shows finer sampling (20× improvement) of the same micro-object by the nanophotonic lens array. Since the focal length of the nanophotonic lens array was voltage dependent, it was also possible to get fine images in the focal plane without fine movement of the microscope objective. This makes optical alignment very simple. Figure 4a shows a section of elemental images captured using the nanophotonic lens array at 1.1 V_{rms}, where each lenslet produced an elemental image of 5 μm radius.

From classical diffraction theory[18] it is well-known that as the lens size decreases, diffraction effects increase and hence reduce resolution. The small aperture (radius 5 μm) and short focal length (13 μm at an applied voltage of 1.1 V_{rms}) associated with the nanophotonic lens array therefore greatly reduces the resolution limitation due to diffraction. The short focal length also has the additional advantage of increasing the field of view of the lenslets. The resolution limitation due to the diffraction could also be further enhanced (beyond Abbe diffraction limit) with yet smaller size lenses (diameter of the order of 1 μm or less) whose focal lengths are close to near field and before diffraction effects predominate.[21,22]

The elemental images were recorded in real time on a high-resolution CMOS camera (EO-10012C $^1/_2$ in. CMOS Color GigE), with pixel resolution 3840 × 2748 and pixel size of 1.67 × 1.67 μm. For the 3D image reconstruction, the recorded elemental images were displayed using a conventional LCD monitor (Silicon Graphics 1600SW, dot pitch 0.23 mm), to which was attached a large lens array. The large lens array was made of two sheets of lenticular cylindrical lenses (10 LPI acrylic sheet with refractive index 1.49) crossed at right angles and sandwiched together. The focal length of the resulting spherical lens array was experimentally measured as 3.9 mm. Each elemental image was represented by 11 × 11 pixels in the display stage. The separation between the large lens array and the display stage was 4 mm from the center of the lens array which was more than the focal length of the fabricated lenticular lens array. This enabled the reconstruction of a real 3D image. The 3D microscope operated in real time.

The viewing angle (Ω) was calculated to be 28° from $\Omega = 2\tan^{-1}(P/2g)$,[10] where P is the pitch of the lenticular lens array and g is the separation between the display and the lenticular lens array. Figure 4b shows the optically reconstructed 3D image observed in front of the display from four different viewing

angles. As the observation direction changes, the perspective of the 3D image displayed in space varies continuously, thus demonstrating the 3D nature of the display with full parallax. The viewing angle was also measured experimentally as 30°, matching with the theoretically obtained value. Although high resolution was achieved in the pickup stage using the nanophotonic lens array, the resolution of the reconstructed 3D image was limited by both the pitch and the relatively poor optical quality of the plastic lenticular lens array. One pixel in the reconstructed 3D image was 2.5 mm (the pitch of lenticular lens array). For further improvement in 3D image clarity, the pixel size could be reduced through use of a higher resolution LCD display or projector together with a lens array with fewer distortions and aberrations.[23]

In summary, a real-time high-resolution 3D microscope for analyzing micro-objects has been demonstrated, by integrating nanotechnology and integral imaging techniques. The 3D microscope can be used for imaging biological samples using a submicrometer pitch nanophotonic lens array enabling nanometer sampling of the specimen. The orthoscopic to pseudoscopic conversion[24] can be done computationally in real time.

■ ASSOCIATED CONTENT

Supporting Information. Video showing 3D motion. This material is available free of charge via the Internet at http://pubs.acs.org.

■ AUTHOR INFORMATION

Corresponding Author
*E-mail: tdw13@cam.ac.uk.

■ ACKNOWLEDGMENT

The authors thank the UK−India Education and Research Initiative (UKIERI) and the Cambridge Commonwealth Trust (CCT) for research studentship funding. The authors also thank Stephen Morris, Haider Butt, and Damian Gardiner for fruitful discussions. Thanks to CambridgeSens for a research grant through network grant innovation competition.

■ REFERENCES

(1) Shaevitz, Joshua W. *Nat. Methods* **2008**, *5*, 471–472.
(2) Kyu, Y. H.; Katrin, I. W.; Eva, R.; Fedor, J.; Christian, E.; Stefan, W. H. *Nano Lett.* **2009**, *9* (9), 3323–3329.
(3) Ersen, O.; Werckmann, J.; Houllé, M.; Ledoux, M.-J.; Pham-Huu, C. *Nano Lett.* **2007**, *7* (7), 1898–1907.
(4) Sun, Y.; Dawicki McKenna, J.; Murray, J. M.; Ostap, E. M.; Goldman, Y. E. *Nano Lett.* **2009**, *9* (7), 2676–2682.
(5) Macpherson, J. V. *Nat. Nanotechnol.* **2011**, *6*, 84–85.
(6) Jiang, Huaidong; Song, C.; Chen, C.-C.; Xu, R.; Raines, K. S.; Fahimian, B. P.; Lu, C.-H.; Lee, T.-K.; Nakashima, A.; Urano, J.; Ishikawa, T.; Tamanoi, F.; Miao, J. *Proc. Natl. Acad. Sci. U.S.A.* **2010**, *107*, 11234–11239.
(7) Gopinathan, U.; Pedrini, G.; Javidi, B.; Osten, W. *J. Disp. Technol.* **2010**, *6*, 479–483.
(8) Hell, S. W.; Schmidt, R.; Egner, A. *Nat. Photonics* **2009**, *3*, 381–387.
(9) Lippmann, M. G. *J. Phys. (Paris)* **1908**, *7*, 821–825.
(10) Okano, F.; Hoshino, H.; Arai, J.; Yuyama, I. *Appl. Opt.* **1997**, *36*, 1598–1603.
(11) Hoshino, H.; Okano, F.; Isono, H.; Yuyama, I. *J. Opt. Soc. Am. A* **1998**, *15*, 2059–2065.
(12) Erdmann, L.; Gabriel, K, J. *Appl. Opt.* **2001**, *40*, 5592–5599.
(13) Okui, M.; Arai, J.; Nojiri, Y.; Okano, F. *Appl. Opt.* **2006**, *45*, 9132–9139.
(14) Okano, F.; Arai, J.; Hoshino, H.; Yuyama, I. *Opt. Eng.* **1999**, *38*, 1072–1077.
(15) Jang, J. S.; Javidi, B. *Opt. Lett.* **2004**, *29*, 1230–1232.
(16) Javidi, B.; Moon, I.; Yeom, S. *Opt. Express* **2006**, *14*, 12096–12108.
(17) Lim, Y. T.; Park, J. H.; Kwon, K. C.; Kim, N. *Opt. Express* **2009**, *17*, 19253.
(18) Born, M. Wolf, E. *Principles of Optics*, 6th ed.; Pergamon: Oxford, 1980.
(19) Wilkinson, T. D.; Wang, X.; Teo, K. B. K.; Milne., W. I. *Adv. Mater.* **2008**, *20*, 363.
(20) Milne, W. I; et al. *Diamond Relat. Mater.* **2003**, *12*, 422–428.
(21) Lee, J. Y.; et al. *Nature* **2009**, *460*, 498–501.
(22) Mason, D. R.; Jouravlev, M. V.; Kim, K. S. *Opt. Lett.* **2010**, *35*, 2007–2009.
(23) Arai., J.; Okano, F.; Kawakita., M.; Okui., M.; Haino., Y.; Yoshimura., M.; Furuya., M.; Sato., M. *J. Disp. Technol.* **2010**, *6*, 422–430.
(24) Jang, J. S.; Javidi, B. *Opt. Eng.* **2003**, *42*, 1869–1870.